Structure Determinations of $La_2O_2CO_3$-II and the Unusual Disordered Phase $La_2O_{2.52}(CO_3)_{0.74}Li_{0.52}$ Using Powder Diffraction

J. PAUL ATTFIELD[*,1] AND GÉRARD FÉREY†

Chemical Crystallography Laboratory, University of Oxford, 9 Parks Road, Oxford, OX1 3PD, United Kingdom, and †Laboratoire des Fluorures, UA CNRS 449, Faculté des Sciences, Université du Maine, Route de Laval, 72017 Le Mans Cédex, France

The crystal structures of $La_2O_2CO_3$-II and a novel lithium-containing derivative, "Li–$La_2O_2CO_3$-II," have been solved from powder X-ray diffraction data. They adopt the $Nd_2O_2CO_3$-II structure in which disordered carbonate groups lie between neodymium oxide layers. It was not possible to locate the lithium or determine accurately the stoichiometry of Li–$La_2O_2CO_3$-II from the X-ray data, and so this structure has also been refined using time-of-flight powder neutron diffraction data. This shows the composition to be $La_2O_{2+2x}(CO_3)_{1-x}Li_{2x}$ with $x = 0.26(1)$. The structural consequences of the lithium incorporation are that $(CO)^{2+}$ units are lost from some carbonate groups, resulting in the displacement of one of the remaining two oxygens, and Li^+ cations occupy bicapped trigonal prismatic cavities in the oxide sublattice. © 1989 Academic Press, Inc.

Introduction

We recently reported diffraction evidence for a new phase $La_4Li_2O_7$, which has an oxygen-deficient K_2NiF_4 structure (1). Subsequent attempts to prepare a pure sample of this phase resulted in the formation of a new compound when mixtures of La_2O_3 and Li_2CO_3 were heated below 550°C in air. This polycrystalline material was found to be structurally related to $La_2O_2CO_3$-II (2), a compound which does not appear to be susceptible to lithium insertion or substitution, and so we have characterized the new phase ("Li–$La_2O_2CO_3$-II") and $La_2O_2CO_3$-II by X-ray and neutron diffraction.

Experimental

White $La_2O_2CO_3$-II was prepared by adding excess sodium bicarbonate solution to a solution of lanthanum nitrate. The precipitate was washed with water and acetone, and heated at 530–550°C for 8 days. The diffraction pattern of this material agreed with the reported pattern (2), and the refined hexagonal cell parameters are $a = 4.077(1)$ Å and $c = 15.958(4)$ Å.

A lithium-containing form of this compound ("Li–$La_2O_2CO_3$-II") was produced when a 2:1 mixture of La_2O_3 and Li_2CO_3 was heated at 550°C in air. After 11 days, all of the La_2O_3 had reacted and the X-ray diffraction pattern showed that only an $La_2O_2CO_3$-II type phase, with $a = 4.061(1)$ Å and $c = 16.238(4)$ Å, and a small amount of Li_2CO_3 were present. Heating La_2O_3 in

[1] To whom correspondence should be addressed.

air at the same temperature resulted in the slow formation of La$_2$O$_2$CO$_3$-II and no intermediate phases were observed.

Long X-ray powder diffraction scans of flat plate samples of both materials were performed for structure determination, using Cu$K\alpha$ radiation. The pattern of La$_2$O$_2$CO$_3$-II was recorded between 5 and 140° 2θ on a Philips PW1380 diffractometer counting for 25 sec per 0.04° step. The profile of Li–La$_2$O$_2$CO$_3$-II was collected in the range 10–150° 2θ on a Siemens D501 diffractometer with a count time of 16 sec per 0.04° step.

The time-of-flight (TOF) neutron diffraction pattern of the same Li–La$_2$O$_2$CO$_3$-II sample was recorded on the POLARIS (3) spectrometer at ISIS, Rutherford-Appleton Laboratory, UK. The sample was held in a cylindrical, 8-mm-radius vanadium can and data were collected at room temperature for 3 hr, during which a total proton beam charge of 200 μA hr was passed. The pattern was recorded between 0 and 20 msec in 7-μsec intervals by the time-focused detector bank at $2\theta = 150°$, corresponding to a 0–3.2 Å d-space range. The spectrum of a vanadium powder was also recorded and fitted by a polynomial function. This curve was used to normalize the Li–La$_2$O$_2$CO$_3$-II data.

Structure Determinations and Refinements

The X-ray diffraction patterns of both samples were indexed on hexagonal cells, and the reflection condition hhl: $l = 2n$ showed the space group to be $P6_3/mmc$ or one of its subgroups. Integrated peak intensities were extracted by a profile fitting method described elsewhere (4) and converted to $|F_{hkl}|^2$'s. These were used in a Patterson synthesis from which La was located, and difference Fourier maps revealed the positions of O(1) and O(2). However, it was not possible to locate the remaining atoms from the difference

Fourier map, and so several trial models were fitted to the profiles using a modified Rietveld program (4, 5). The only one to give a good fit and a stable refinement was with C and O(3) on (x, $2x$, $\frac{1}{4}$). These two sites are $\frac{1}{3}$ occupied in stoichiometric La$_2$O$_2$CO$_3$-II. This starting model was refined for both sets of data, using neutral atom scattering factors (6) and anisotropic thermal parameters for La. The asymmetric 002 peak was excluded from both refinements, and small contributions due to La$_2$O$_2$CO$_3$-I [2] and Li$_2$CO$_3$ were excluded from the refinements of La$_2$O$_2$CO$_3$-II and Li–La$_2$O$_2$CO$_3$-II, respectively. As it is not evident how the stoichiometry of La$_2$O$_2$CO$_3$-II changes with Li insertion, we assumed that equal numbers of C and O(3) are lost from the Li–La$_2$O$_2$CO$_3$-II structure on lithiation. This gives the stoichiometry La$_2$O$_{2+2x}$(CO$_3$)$_{1-x}$Li$_{2x}$, which we will henceforth write as La$_2$O$_4$(CO)$_{1-x}$Li$_{2x}$ for convenience. x refined to a value of 0.15(1) but it was not possible to locate the lithium from the final Fourier difference map. Observed, calculated, and difference X-ray diffraction profiles for Li–La$_2$O$_2$CO$_3$-II are shown in Fig. 1.

The TOF neutron diffraction data for Li–La$_2$O$_2$CO$_3$-II in the range 3500–17000 μsec, equivalent to sin $\theta/\lambda = 0.18$–0.89 Å^{-1}, were fitted by a profile fitting program employing CCSL subroutines (7). Neutron scattering lengths were taken from Sears' report (8) and used to fit the Li–La$_2$O$_2$CO$_3$-II model in $P6_3/mmc$. Variation of the site occupancies showed that vacancies were present on the O(2), O(3), and C positions and the "observed" and calculated $|F_{hkl}|$'s derived from this refinement were used to construct a difference Fourier map. This revealed a large volume of negative scattering density around ($\frac{2}{3}$, $\frac{1}{3}$, $\frac{1}{4}$), which was taken to be the Li position (lithium has a negative neutron scattering length), and a small positive peak close to O(2) at (0.26, 0.13, 0.13) that was assumed to be an additional oxygen site,
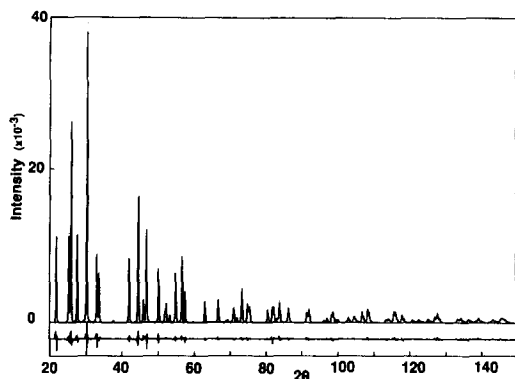
FIG. 1. Observed (points), calculated (full line), and difference X-ray diffraction profiles for the Li–La$_2$O$_2$CO$_3$-II sample.

FIG. 2. Observed (points), calculated (full line), and difference TOF neutron diffraction profiles for Li–La$_2$O$_2$CO$_3$-II, with reflection positions marked.

O(4). The occupancies of O(3), C, and Li were varied subject to the stoichiometry given above; the values for the O(3) and C sites were not found to differ significantly and so were constrained to be equal in the final refinements. The refined occupancy of the O(4) site was found to be approximately equal to the number of O(2) vacancies, and so the total occupancies of these two sites were constrained to sum to unity. Varying the O(2) temperature factor anisotropically suggested that this atom was disordered in the xy plane, and so O(2) was subsequently refined on $(x, 2x, z)$ to model the displacements. Final observed, calculated, and difference TOF profiles are shown in Fig. 2. Results of all three refinements are given in Table I and bond distances and angles are presented in Table II.

Discussion

The structure determined for La$_2$O$_2$CO$_3$-II from powder X-ray diffraction (Fig. 3) is the same as the structure found for a hydrothermally grown crystal of Nd$_2$O$_2$CO$_3$-II by X-ray methods (9) and is similar to a model proposed by Turcotte *et al.* (10). The structure is based on LaO$_2$ layers parallel to (001), identical to those in the A-type La$_2$O$_3$
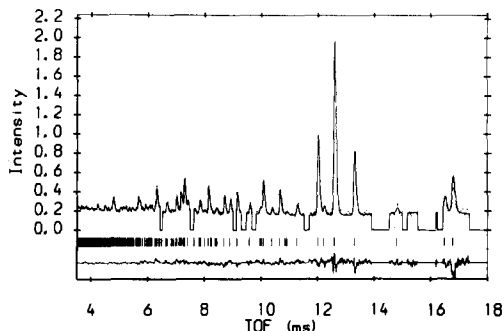
structure. The dimensions of these layers are characterized by the cell parameters of the trigonal La$_2$O$_3$ structure, which are $a = 3.94$ Å and $c = 6.13$ Å, and the corresponding distances in La$_2$O$_2$CO$_3$-II are 4.08 and 5.73 Å, respectively. These LaO$_2$ layers are stacked directly upon one another in La$_2$O$_3$ and share planes of oxygens, but in La$_2$O$_2$CO$_3$-II, the LaO$_2$ layers are separated

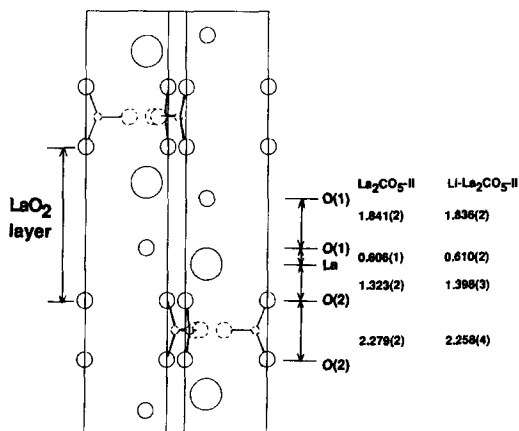FIG. 3. A projection of the La$_2$O$_2$CO$_3$-II structure close to the (110) plane with the hexagonal unit cell marked and the ⅓ occupied O(3) and C sites shown as broken circles. (La/O/C are the large/medium/small circles.) The interplanar distances from the X-ray refinements of the La$_2$O$_2$CO$_3$-II and Li–La$_2$O$_2$CO$_3$-II structures are marked.

TABLE I

RESULTS OF THE POWDER X-RAY REFINEMENTS OF (a) $La_2O_2CO_3$-II AND (b) Li–$La_2O_2CO_3$-II AND (c) THE POWDER NEUTRON REFINEMENT OF Li–$La_2O_2CO_3$-II, WITH ESDS IN PARENTHESES

	(a)	(b)	(c)
Number of profile points	2720	2960	1744
Number of *hkl*'s	109	121	308
$\sin \theta/\lambda$ range	0.12–0.61	0.12–0.62	0.18–0.89
R factors (%)[a]			
R_{WP}	8.7	10.7	4.0
R_P	7.5	9.4	5.3
R_{NUC}	2.9	2.9	10.2
Cell parameters (Å)			
a	4.0755(6)	4.0582(4)	4.0580(1)
c	15.957(1)	16.2211(6)	16.2219(1)
Cell volume (Å³)	229.5(1)	231.36(7)	231.34(1)

Atomic parameters in $P6_3/mmc$ (No. 194)[b]

	Atom	Site	*x*	*y*	*z*	B_{ISO}	B_{11}	B_{33}	Occupancy
(a)	La	4(f)	⅓	⅔	0.09570(4)	0.256	0.224(2)	0.336(1)	
(b)					0.09422(5)	0.506	0.438(2)	0.674(1)	
(c)					0.0943(1)	0.55	0.45(4)	0.82(9)	
(a)	O(1)	4(f)	⅓	⅔	0.5577(3)	1.2(1)			
(b)					0.5566(4)	1.0(2)			
(c)					0.5569(2)	0.51	0.33(5)	1.2(1)	
(a)	O(2)	4(e)	0	0	0.1786(4)	3.0(2)			
(b)					0.1804(7)	3.3(3)			
(c)		12(k)	−0.0341(6)	−0.0681(9)	0.1755(4)	0.25(6)			0.266(4)
(a)	O(3)	6(h)	0.235(2)	0.470(3)	¼	2.0(4)			⅓
(b)			0.228(2)	0.456(3)		2.1(6)			0.282(7)
(c)			0.228(1)	0.456(2)		0.25(6)			0.247(5)
(c)	O(4)	12(k)	0.261(6)	0.131(3)	0.133(1)	0.25(6)			0.067(4)
(a)	C	6(h)	0.040(6)	0.080(9)	¼	2.1(8)			⅓
(b)			0.058(5)	0.116(7)		2.1(6)			0.282(7)
(c)			0.0470(9)	0.094(1)		0.25(6)			0.247(5)
(c)	Li	2(d)	⅔	⅓	¼	11(3)			0.52(1)

[a] *R* factors are defined in Ref. (5).

[b] The parameters were constrained; (b) O(3): B_{ISO} = C: B_{ISO}, O(3): occupancy = C: occupancy; (c) O(2): B_{ISO} = O(3): B_{ISO} = O(4): B_{ISO} = C: B_{ISO}, O(3): occupancy = C: occupancy, O(2): occupancy + O(4): occupancy = ⅓, (6 × C: occupancy) + Li: occupancy = 2.

from each other by 2.28 Å and there is a 180° rotation between successive layers. This gives rise to trigonal prismatic cavities between layers defined by three O(2), O(2') pairs at (*x*, *y*, *z*), (*x*, *y*, ½ − *z*). The two triangular faces of the prisms are capped by a pair of oxygens or lanthanums. CO(3) groups occupy the lanthanum-bicapped cavities such that C is bonded to one of the O(2), O(2') pairs and O(3) is close to the center of the cavity and coordinates to the two capping lanthanums. Hence the lanthanum is eight-coordinate (bicapped octahedron) in $La_2O_2CO_3$-II, but seven-coordinate (monocapped octahedron) in La_2O_3. The positional disorder of the carbonate

TABLE II

INTERATOMIC DISTANCES (Å) AND ANGLES (°) FROM THE POWDER X-RAY REFINEMENTS OF (a) $La_2O_2CO_3$-II AND (b) $Li-La_2O_2CO_3$-II AND (c) THE POWDER NEUTRON REFINEMENT OF $Li-La_2O_2CO_3$-II, WITH ESDS IN PARENTHESES

		(a)	(b)	(c)
La–O(1a)	(×3)	2.430(1)	2.421(2)	2.420(1)
La–O(1b)		2.448(5)	2.447(7)	2.452(4)
La–O(2)	(×3)	2.699(3)	2.728(6)	(×2) 2.593(5)
				2.899(4)
La–O(3)		2.558(3)	2.633(4)	2.632(3)
La–O(4)				(×6) 2.14(2)
C–O(2)	(×2)	1.17(1)	1.20(2)	1.336(6)
C–O(3)		1.38(4)	1.19(4)	1.275(7)
Li–O(2c)	(×6)			2.426(4)
Li–O(2)	(×12)			2.751(4)
Li–O(3)	(×6)			2.075(6)
Li–O(4)	(×6)			2.37(1)
Li–C	(×6)			2.196(5)
O(1)–O(4d)				1.88(2)
O(2)–O(2b)		2.28(1)	2.26(2)	2.42(1)
O(2)–O(3)	(×2)	2.012(9)	1.96(1)	2.205(6)
O(2)–C–O(2b)		152(3)	140(3)	129.5(5)
O(2)–C–O(3)	(×2)	104(2)	110(2)	115.3(2)

Note. The numbers of equivalent bonds shown do not take the partial occupancies of some sites into account. Symmetry operators: a: $y, x, z - \frac{1}{2}$; b: $x, y, \frac{1}{2} - z$; c: $-y, x - y, z$; d: $x - y, x, \frac{1}{2} + z$.

groups in $La_2O_2CO_3$-II is unusual as each $CO(2)O(2')O(3)$ group occupies one of three possible orientations around an axis passing through O(2) and O(2'). However, the orientation of each carbonate group is influenced by neighboring groups as each O(2), O(2') pair is connected to only one CO(3) group, and only one CO(3) group is present per lanthanum-bicapped trigonal prismatic cavity. Hence, there is no disorder in the primary coordination spheres of La, C, or any of the O's, although disorder is present in the second spheres. The gain in lattice energy from further, long range ordering of the carbonate groups in $La_2O_2CO_3$-II would be small in comparison to the loss of the entropy contribution to the free energy, and so long range order of the carbonates is not observed.

The carbonate group in $La_2O_2CO_3$-II is apparently very distorted, with unrealistically short O(2)–O(3) distances. This may be due to inaccuracies in the x coordinates for C and O(3) or to disorder of O(2) which was not fitted in this model.

The changes in the unit cell parameters when $La_2O_2CO_3$-II is prepared in the presence of lithium carbonate indicate that lithium has been incorporated into the structure. The powder X-ray refinement of $Li-La_2O_2CO_3$-II does not reveal the position of the inserted lithium but does show that C and O(3) vacancies consistent with the composition $La_2O_4(CO)_{1-x}Li_{2x}$ are present. However, the refined value of $x = 0.15(1)$ cannot be regarded as more than 20% accurate, in view of the low X-ray scattering powers of carbon and oxygen. Slight differences in the powder X-ray structures of $La_2O_2CO_3$-II and $Li-La_2O_2CO_3$-II are apparent by considering the distances between the planes of atoms parallel to (001), as shown in Fig. 3. These indicate that the increase in c that takes place on lithiation of $La_2O_2CO_3$-II is due to an increase in the distance between successive La and O(2) planes within the LaO_2 layers, rather than between the layers. This seems surprising as both the CO(3) groups are lost and (as the neutron refinement shows) the Li is inserted between the layers, but may be rationalized upon the neutron-refined structure (see later).

The sensitivity of neutrons for light atoms allows a more detailed description of the $Li-La_2O_2CO_3$-II structure to be obtained than with X-rays. The best model for the lithium substitution was found to be that assumed above, and gives the stoichiometry as $La_2O_4(CO)_{0.74(1)}Li_{0.52(1)}$. Li was placed at the center of the oxygen-bicapped prisms between the LaO_2 layers as it was not possible to refine it off this site. However, the large B_{ISO} value, the long Li–O bond distances, and the high coordination number for this site suggest that this is not the minimum energy position for Li^+, but that the lithiums are disordered over several sites within the cage. Refining O(2) off
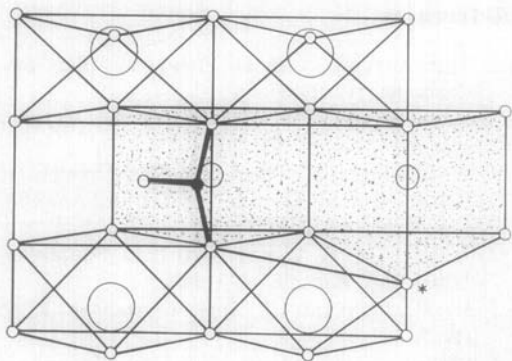
FIG. 4. Disorder in the interlayer region of Li-La₂O₂CO₃-II, projected close to the yz plane for $0 < z < 0.56$. (y horizontal, z near-vertical; La/Li/O are the large/medium/small open circles and C is the small filled circle.) The octahedra around the La³⁺ cation and the trigonal prisms defined by the oxide ions are shown. The loss of a $(CO)^{2+}$ unit from a lanthanum-bicapped trigonal prism results in the displacement of an O^{2-} ion from the O(2) to the O(4) site (marked *) and the incorporation of two Li⁺'s into vacant oxygen-bicapped cavities (speckled).

$(0, 0, z)$ and the greater precision in the co-ordinates of C and O(3) result in a more satisfactory geometry for the carbonate group than those from the two X-ray refinements. The C–O(2) bond is significantly longer than the C–O(3) bond, reflecting the fact that O(2) is coordinated to more cations and so is more ionic than O(3). This provides some justification for describing $La_2O_{2+2x}(CO_3)_{1-x}Li_{2x}$ as $La_2O_4(CO)_{1-x}Li_{2x}$ in order to emphasize the loss of the $(CO)^{2+}$ group on lithium substitution.

The neutron profile refinement also shows that 20% of the oxide anions on the O(2) site are transferred to the O(4) site, which lies between adjacent La and O(2) planes. This reduces the repulsion that would occur between two O^{2-} anions on O(2) and O(2′) sites when the CO(3) group between them is lost. The independently refined O(2) and C/O(3) occupation factors do not differ greatly, indicating that approximately one oxide is displaced from an O(2) to an O(4) site for every CO(3) unit lost. The apparently short distances from the

O(4) site to La and O(1) show that large local displacements of the latter atoms must occur when this site is filled. This results in the difference between the La–O(2) inter-planar distances in the X-ray structures that was noted above, and so the increase in c on lithium substitution in La₂O₂CO₃-II may be ascribed to occupation of the interstitial O(4) site rather than to the insertion of Li or to the loss of CO(3) units. The disorder in Li–La₂O₂CO₃-II is illustrated in Fig. 4.

Although a 2:1 ratio of $La_2O_3 : Li_2CO_3$ was used in the preparation of the Li–La₂O₂CO₃-II sample, substitution occurs only to $x = 0.26(1)$ in $La_2O_4(CO)_{1-x}Li_{2x}$ under the experimental conditions. This limit presumably reflects the greatest amount of disorder tolerable to the La₂O₂CO₃-II structure, above which the LaO₂ layers would collapse together to form La₂O₃.

The insertion of lithium into a compound containing no reducible species and no cations for which Li⁺ can readily substitute is unusual. It reflects the nature of the cavities in the interlayer region of the La₂O₂CO₃-II structure which enables some $(CO)^{2+}$ units to be lost from the lanthanum-bicapped cages, as the charge-compensating Li⁺ cations can be inserted into the oxygen-bicapped trigonal prisms and so support the layer structure. Although this may lead to a loss of lattice energy, the equilibrium

$$La_2O_4(CO) + xLi_2CO_3 \rightleftharpoons$$
$$La_2O_4(CO)_{1-x}Li_{2x} + 2xCO_2$$
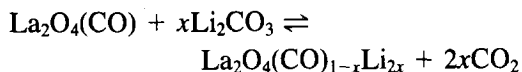
is driven to the right-hand side by the increase in entropy and the low aerial partial pressure of CO_2.

This work shows that it is possible to obtain accurate structural models using powder diffraction data collected with a characteristic X-ray source by profile fitting methods, provided an adequate peak shape function is used (4). The agreement factor $\langle \Delta p / \sigma(\Delta p) \rangle$ (11) between the comparable X-ray and neutron coordinates (those of La, O(1), O(3), and C) for Li–La₂O₂CO₃-II is

0.89. This agreement is very good, especially in view of the low electron density on the C and O(3) sites. However, the sensitivity of neutrons to scattering by light atoms such as C, O, and Li enabled a full structural description to be obtained only with the neutron data. TOF data such as that collected on POLARIS is especially good for such refinements, as the high flux enables a good pattern to be collected rapidly, the resolution ($\Delta d/d \sim 5 \times 10^{-3}$) results in an reproducible peak shape, and the large $\sin \theta/\lambda$ range allows reliable thermal parameters and occupation factors to be obtained from the refinement.

Acknowledgments

References

1. J. P. ATTFIELD AND G. FÉREY, *J. Solid State Chem.* **80**, 112 (1989).
2. J. O. SAWYER, P. CARO, AND L. EYRING, *Monatsch. Chem.* **103**, 333 (1972).
3. W. G. WILLIAMS, "Polarisation Spectrometers for Pulsed Neutron Sources," Rutherford-Appleton Lab. Report NDR/P1/84 (1984).
4. A. LE BAIL, H. DUROY, AND J. L. FOURQUET, *Mater. Res. Bull.* **23**, 447 (1988).
5. H. M. RIETVELD, *J. Appl. Crystallogr.* **2**, 65 (1969).
6. "International Tables for X-ray Crystallography," Vol. IV, Kynoch Birmingham (1974).
7. P. J. BROWN AND J. MATTHEWMAN, "The Cambridge Crystallography Subroutine Library- Mark 3 User's Manual," Rutherford-Appleton Lab. Report 87-010 (1987).
8. V. F. SEARS, "Thermal Neutron Scattering Lengths and Cross-sections for Condensed Matter Research," Chalk River Nuclear Lab.- Internal Report AECL-8490 (1984).
9. A. N. CHRISTENSEN, *Acta Chem. Scand.* **24**, 2440 (1970).
10. R. P. TURCOTTE, J. O. SAWYER, AND L. EYRING, *Inorg. Chem.* **8**, 238 (1969).
11. J. P. ATTFIELD, A. K. CHEETHAM, D. E. COX, AND A. W. SLEIGHT, *J. Appl. Crystallogr.* **21**, 452 (1988).